

# Morphology and Properties of Nylon6 and High Density Polyethylene Blends in Absence and Presence of Nanoclay

Sumana Mallick, B. B. Khatua

Materials Science Centre, Indian Institute of Technology, Kharagpur 721 302, India

Received 12 August 2010; accepted 11 October 2010

DOI 10.1002/app.33580

Published online 18 February 2011 in Wiley Online Library (wileyonlinelibrary.com).

**ABSTRACT:** The morphology and properties of nylon6/HDPE blends without and with nanoclay has been reported. Scanning electron microscopy study of the (70/30 w/w) nylon6/HDPE blends with small amount (0.1 phr) of nanoclay indicated a reduction in the average domain sizes ( $D$ ) of dispersed HDPE phase and hence better extent of mixing compared to the blend without any nanoclay. X-ray diffraction study and transmission electron microscopy revealed that nanoclay layers were mostly located in nylon6 matrix of the (70/30 w/w) nylon6/HDPE blend. However, the same effect of nanoclay on the morphology was not observed in (30/70 w/w) nylon6/HDPE blend where HDPE became the matrix. In (30/70 w/w) nylon6/HDPE blend, addition of nanoclay increased

the  $D$  of dispersed nylon6 domains by preferential location of the clays in side the nylon6 domains. Thus, the clay platelets in the matrix phase acted as barrier that restricted the coalescence of dispersed domains during melt-mixing. Addition of PE-g-MA in both the compositions of nylon6/HDPE blend effectively reduced the  $D$  of dispersed phases. Storage modulus and thermal stability of the blend were improved in presence of small amount of clay, whereas addition of PE-g-MA lowered the mechanical and thermal properties of the blends. © 2011 Wiley Periodicals, Inc. *J Appl Polym Sci* 121: 359–368, 2011

**Key words:** clay; nylon6; nanocomposites; exfoliation; barrier; coalescence

## INTRODUCTION

Blending two or more polymers is an effective way to obtain new polymeric materials with improved performance properties than those of the neat polymers. Unfortunately, most polymer pairs are immiscible due to their unfavorable enthalpy changes, and thus form phase separated morphology in the blends. Generally, addition of block or graft copolymers as compatibilizer during mixing reduces the interfacial tension and improves the adhesion between the phases by making entanglement or bridging the polymer chains near the interface of the blend.<sup>1–5</sup> However, synthesis of various blocks or graft copolymers depending on the blend components limits the use of polymeric compatibilizer in immiscible polymer blends.

High density polyethylene (HDPE) and nylon6 represent two important classes of polymers. Because of low cost, high barrier properties to moisture, good optical properties, and ease of processing, HDPE is widely employed. However, its high permeability to

organic solvents and vapor limits its potential. On the other hand, Nylon6 is an engineering thermoplastic with high strength, wear, and heat resistance properties. It is, however, relatively expensive and has poor impact strength and moisture resistance properties. Thus, blends of HDPE with nylon6 have often been prepared to retain the most desirable properties of both the polymers, while avoiding their drawbacks. However, addition of graft copolymer as compatibilizer in immiscible nylon6/HDPE blend often reduces the stiffness and hence, the modulus of this blend.

In recent years, several research groups have shown that organically modified clay could play the role of compatibilizer in immiscible polymer blends.<sup>6–16</sup> Khatua et al.<sup>6</sup> reported that presence of exfoliated clay platelets in nylon6 phase prevented the coalescence of dispersed poly(ethylene-*ran*-propylene) rubber (EPR) domains during mixing that decreased the average domain sizes ( $D$ ) of EPR phase in (80/20 w/w) nylon 6/EPR blend. Hong et al.<sup>7</sup> showed a decrease in  $D$  of HDPE in poly(butylene terephthalate)/high density polyethylene (PBT/HDPE) blend in presence of clays (1–3 phr) dispersed in the PBT matrix. The presence of clay in the matrix phase changed the viscosity ratio of the polymers and suppressed the coalescence of dispersed domains in the blend. Gelfer et al.<sup>8</sup> reported that preferential location of 10 wt % nanoclay in poly(methyl methacrylate) (PMMA) phase increased the

Correspondence to: B. B. Khatua (khatuabb@matssc.iitkgp.ernet.in).

Contract grant sponsor: Department of Science and Technology (DST), India.

viscosity of PMMA in (50/50 w/w) PS/PMMA blend that reduced the dispersed PS domain sizes. Wang et al.<sup>9</sup> reported significant reduction of PS domain sizes in (70/30 w/w) PP/PS blend with 5 wt % of clay. They assumed that cointercalation of both polypropylene (PP) and polystyrene (PS) chains inside the same clay galleries played the role of compatibilizer for the blend, similar to that of a block copolymer. Sinha Ray and Bousmina<sup>10,11</sup> showed that presence of 3 wt % organoclay improved the miscibility between polycarbonate (PC) and PMMA in (40/60 w/w) PC/PMMA blends. Yoon and co-workers<sup>12</sup> showed that selective dispersion of 4 phr clay in acrylonitrile butadiene styrene (ABS) phase decreased the droplet sizes of PP in (70/30 w/w) ABS/PP blend. They explained it in terms of decrease in viscosity ratio of polypropylene (PP) and ABS polymers in presence of clay. Gcwabaza et al.<sup>13</sup> reported that intercalation of both PP and poly(butylene succinate) (PBS) chains into the same silicate layers at the interface and change in viscosity ratio of the polymers resulted in a homogeneous dispersion of PBS domains in (70/30 w/w) PP/PBS blends with various amount of clay (0.5–5 wt %). Mehta et al.<sup>14</sup> reported that increase in melt viscosity of PP phase by selective intercalation of clay (0.6–6.7 wt %) in the PP phase decreased the dispersed EPR domain sizes in (70/30 w/w) PP/EPR blends. Kelnar et al.<sup>15</sup> showed that presence of 5 wt % nanoclay in (90/10 w/w) PA6/PS blends resulted in a finer distribution of PS phase and better interfacial adhesion between the polymers. Calcagno et al.<sup>16</sup> showed that the average domain size of dispersed polyethylene terephthalate (PET) phase in (70/30 w/w) PP/PET blend was increased in presence of 2 wt % of nanoclay. The dispersion of nanoclay inside the PET phase increased the viscosity ratio of the dispersed phase and the matrix polymer that led to an increase in the dispersed domain sizes. Mantia and co-workers<sup>17</sup> reported the formation of highly elongated PA6 domains in HDPE matrix when (75/25 w/w) HDPE/PA6 blend with 5phr of organoclay was immediately cool from the extrusion temperature. Interestingly, when the extruded pellets were compressed between the parallel plates of the rheometer, the morphology became a cocontinuous structure due to the connection of the elongated domains after the melting. Fang et al.<sup>18</sup> have reported a finer dispersion of HDPE phases in (70/30 w/w) PA6/HDPE blends in presence of 1.2 phr nanoclay. The clay platelets located in the PA6 phase and at the interface played the role of a coupling agent in the blend.

In summary, reports on polymer blend-clay nanocomposites indicated a reduction in dispersed domain sizes due to selective localization of clays in the matrix phase that lowered the viscosity ratio of

dispersed/matrix phases in the blends. Now one can raise an important question: is it possible to reduce the domain sizes of disperse phase in immiscible polymer blends by using clay where viscosity increment of the matrix polymer by the clay is almost negligible? To address this, we investigated the morphology of (70/30 w/w) nylon6/HDPE blend in presence of small amount (0.1 phr) of clay (Cloisite 20A). The rationale behind choosing nylon6/HDPE blend was that nylon6 is well-known to exfoliate cloisite 20A, whereas HDPE chains intercalate the silicate layers.<sup>19</sup> Thus, in nylon6/HDPE blend-clay nanocomposites, small amount (0.1 phr) of clay could selectively be dispersed in nylon6 phase because of its favorable interaction with nylon6. Thus, the average domain size ( $D$ ) of HDPE phase in the (70/30 w/w) nylon6/HDPE blend with various clay loadings (0–5 phr) was investigated through SEM analysis and a plausible mechanism behind the compatibilization effect of the clay was proposed considering the location of the clay in the blend.

## EXPERIMENTAL DETAILS

### Materials used

Commercial grade nylon6 (Gujlon M28RC, density: 1.14 g mL<sup>-1</sup>, MFI: 28 g/10 min at 230°C and 2.16-kg load) was obtained from GSFC, Gujarat, India. High density polyethylene (HDPE, M5018L, MFI 19 g/10 min at 150°C and 2-kg load, density 0.95 g mL<sup>-1</sup>) was obtained from Haldia Petrochemicals, Haldia, India. Maleic anhydride grafted polyethylene (PE-g-MA, A-C® 575P, density 0.92 g cm<sup>-3</sup>, maleic anhydride content: <0.5 wt %) was purchased from Honeywell, USA. Cloisite 20A, a modified montmorillonite, was supplied by Southern Clay, USA. It is a montmorillonite modified with dimethyl dihydrogenated tallow ammonium to increase the  $d$ -spacing of Na<sup>+</sup>-montmorillonite. The cation exchange capacity (CEC) of Cloisite 20A is 95 mequiv/100 g of clay. Hereafter, Cloisite 20A is referred to as the clay.

### Preparation of nylon6/HDPE blends

The blends of Nylon6 and HDPE were prepared at three different compositions (70/30, 30/70, and 99/1 w/w) with various amount [0–5 phr (parts per hundred resin)] of PE-g-MA and (or) clay by melt mixing in an internal mixer (Brabender, mixing chamber capacity: 20 cm<sup>3</sup>, counter rotating screws; S. C. Dey, Kolkata, India) at 250°C and 60 rpm for 20 min. To avoid moisture induced thermal degradation, all polymers and the clay were dried in a vacuum oven at 80°C for 36 h before the melt mixing. Finally, the blends were compression molded in a hot press at 250°C under constant pressure (20 MPa) and cooled

to room temperature by air cooling. The compression molded samples of desired shapes were taken for further characterizations.

## CHARACTERIZATION OF THE BLENDS

### Morphology study by SEM

The phase morphology of the nylon6/HDPE blends was studied with scanning electron microscope (SEM, VEGA II LSU, TESCAN, Czech Republic), operated at an accelerating voltage of 10 kV. The blend specimens were carefully broken under liquid nitrogen atmosphere. Then, the specimens were coated with a thin layer of gold to avoid electrical charging. The SEM images were taken on the fractured surface of the specimens.

The number-average domain diameter ( $D_n$ ) of the dispersed phase was calculated with image analyzer software (Scion Image Analyzer, Scion, USA). The cross-sectional area ( $A_i$ ) of each domain in the SEM micrograph was measured and then converted into the diameter ( $D_i$ ) of a circle having the same cross-sectional area by using the following equations:

$$D_i = 2(A_i/\pi)^{\frac{1}{2}} \quad (1)$$

$$D_n = \frac{\sum N_i D_i}{\sum N_i} \quad (2)$$

where,  $N$  is the number of dispersed domains in the SEM micrograph.

### X-ray diffraction study

The gallery height ( $d$ -spacing) of the pure clay, as well as, that in nylon6/HDPE blends was examined by using a wide angle X-ray diffractometer, (WAXD, Ultima-III, Rigaku, Japan) with nickel-filtered Cu  $K\alpha$  line ( $\lambda = 0.15404$  nm), operated at 40 kV and 100 mA, at a scanning rate of  $0.5^\circ \text{ min}^{-1}$ . The sample-to-detector distance was 400 mm.

### TEM analysis

The location of the clay platelets in nylon6/HDPE blends was studied by transmission electron microscope (HRTEM: JEM-2100, JEOL, Japan), operated at an accelerating voltage of 200 kV. The blend-clay nanocomposite samples were ultra-microtomed at cryogenic condition with a thickness of 60–80 nm. Since the clay has much higher electron density than neat polymers, it appeared dark in TEM images.

### Complex viscosity measurement

A frequency sweep experiment for neat nylon6, HDPE and nylon6/HDPE blends without and with

clay was done at  $210^\circ\text{C}$  under a nitrogen environment by using an Advanced Rheometrics Expansion System (ARES, AR-1000 model, TA Instruments) with parallel plates of 25-mm diameter. The strain amplitude ( $\gamma^0$ ) was 0.03, which lies in the linear viscoelastic regime.

### Dynamic mechanical analysis (DMA)

Thermomechanical properties (storage modulus) of the compression molded blends were measured in tension film mode at a constant vibration frequency of 1 Hz, a temperature range of 40– $130^\circ\text{C}$ , and a heating rate of  $5^\circ\text{C min}^{-1}$  in a nitrogen atmosphere by using a dynamic mechanical analyzer (DMA 2980 model, TA Instruments, USA). The dimension of the specimen was  $30 \times 6.40 \times 0.45 \text{ mm}^3$ .

### Mechanical testing

Tensile measurement of the blends without and with clay was carried out with a universal tensile testing machine (Hounsfield HS 10KS, UK) at room temperature with an extension speed of  $5 \text{ mm min}^{-1}$  and an initial gauge length of 35 mm. Dumb-bell shaped testing samples ( $64 \text{ mm} \times 12.7 \text{ mm} \times 3.2 \text{ mm}$ ) were used for tensile testing with at least 24 h allowed after molding to relax the stresses induced during cooling. The results reported are the average of five measurements for each sample, each with an experimental error of  $\pm 2\%$ .

### Thermogravimetric analysis (TGA)

The thermal stability [(temperature corresponds to 10 wt % ( $T_{10}$ ), 50 wt % ( $T_{50}$ ), and maximum weight loss ( $T_{\text{max}}$ )] of the blends without and with the clay was investigated with thermo gravimetric analysis (TGA-209F, from NETZSCH, Germany). The sample was heated in air atmosphere from room temperature to  $600^\circ\text{C}$  at a heating rate of  $10^\circ\text{C min}^{-1}$ .

## RESULTS AND DISCUSSION

### Morphological analysis

The SEM images of (70/30 w/w) nylon6/HDPE blend with various amounts (0–5 phr) of clay are shown in Figure 1. As observed, in the pure blend [Fig. 1(a)], the HDPE phase dispersed as larger spherical domains in nylon6 matrix. This indicated weak interfacial adhesion between nylon6 and HDPE due to the immiscible nature of the polymers. Addition of small amount of clay in the blend reduced the dispersed domain size ( $D$ ) of HDPE [Fig. 1(b)]. For instance,  $D$  of pure blend ( $2.84 \mu\text{m}$ ) was reduced to  $2.06 \mu\text{m}$  when the blend was

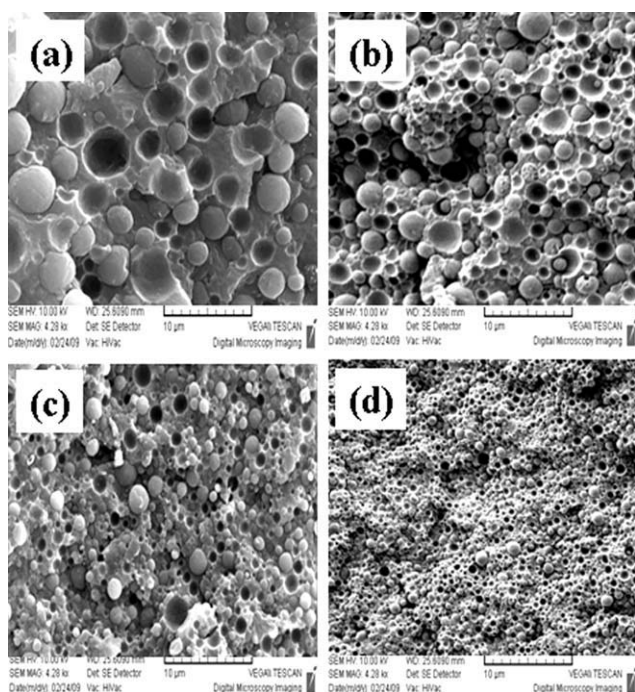


**Figure 1** SEM images of (70/30 w/w) nylon6/HDPE blends with different amount of clay: (a) 0 phr, (b) 0.1 phr, (c) 2 phr, (d) 5 phr. All the images were taken at same magnification, with a scale bar of 10  $\mu\text{m}$ .

formulated with 0.1 phr of clay. With increasing the amount (phr) of the clay, the  $D$  of the blend gradually decreased [Fig. 1(c,d)]. This indicated that the

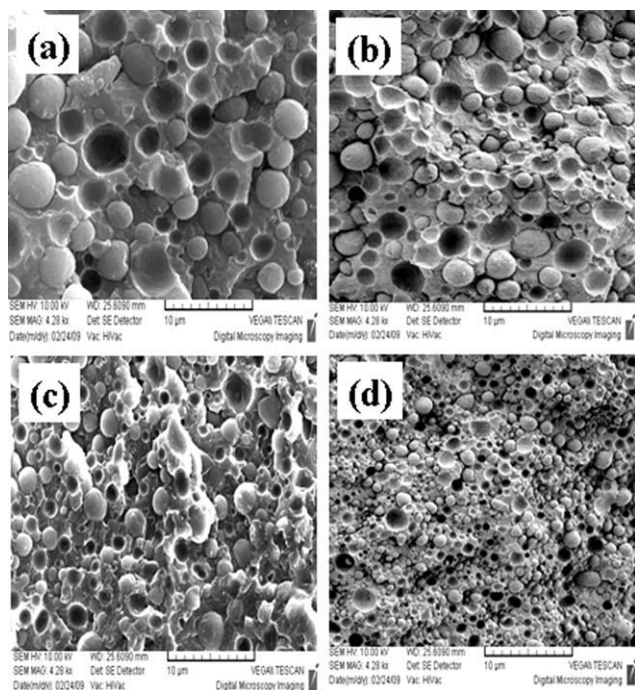


**Figure 2** SEM images of (70/30 w/w) nylon6/HDPE blends with different amount of PE-g-MA: (a) 0 phr, (b) 0.1 phr, (c) 2 phr, (d) 5 phr. All the images were taken at same magnification, with a scale bar of 10  $\mu\text{m}$ .

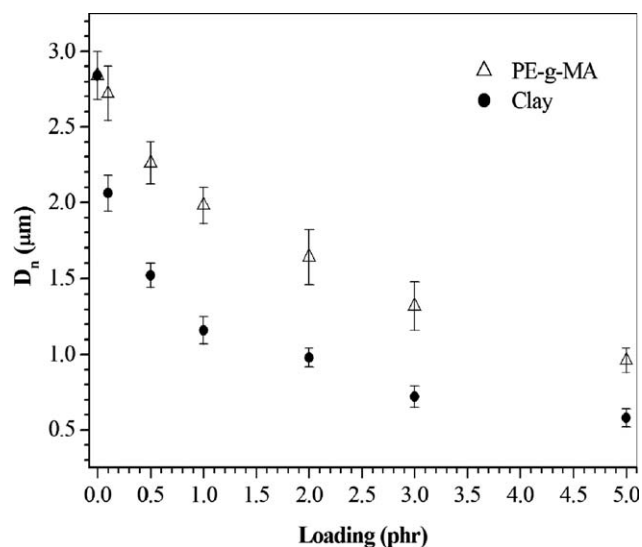


**Figure 3** Plot of  $D_n$  versus loading (phr)  $\Delta$  of clay and PE-g-MA in (70/30 w/w) nylon6/HDPE blend.

clay played an important role in reducing the dispersed domain sizes of nylon6/HDPE blends.

We also prepared (70/30 w/w) nylon6/HDPE blends with various amounts (0–5 phr) of PE-g-MA as reactive compatibilizer to compare decrease in  $D$  of both the systems. From the SEM images (Fig. 2), a decrease in  $D$  of the blend was observed with the addition of PE-g-MA. However,  $D$  of the blend (2.84  $\mu\text{m}$ ) was marginally decreased (2.72  $\mu\text{m}$ ) when 0.1 phr PE-g-MA was added to the blend [Fig. 2(b)]. With the increase in PE-g-MA content, the  $D$  of the blend decreased gradually [Fig. 2(c,d)].

On the basis of the SEM images, the plots of  $D_n$  versus the amount of the clay and PE-g-MA are shown in Figure 3. Interestingly, a rapid decrease in  $D$  of the blend was found at lower amounts (up to 1 phr) of the clay, and then a slow but gradual decrease in  $D$  was observed with further increasing the amount of the clay. The decreasing trend of  $D$  in the blend with the clay content was very similar to the  $D$  of the blend with various amount of PE-g-MA, as shown in Figure 3. However, for certain loading (phr) the decrease in  $D$  of the blend was more in presence of the clay, compared to that with PE-g-MA. This plot of  $D$  versus clay loading was similar to the emulsification curve, which has been reported for an immiscible blend with a block or graft copolymer.<sup>20</sup>

To investigate the role of clay in decreasing the  $D$  of HDPE in (70/30 w/w) nylon6/HDPE blend, we considered the morphology of the clay in neat polymers as well as that in the blend. Figure 4 shows the WAXD profiles of the clay itself and its nanocomposites with nylon6, HDPE, and nylon6/HDPE blends. The clay itself exhibited the characteristic peak at a  $2\theta$  of  $3.62^\circ$  corresponding the  $d$ -spacing of 2.44 nm. The shifting of the clay peak position to lower  $2\theta$

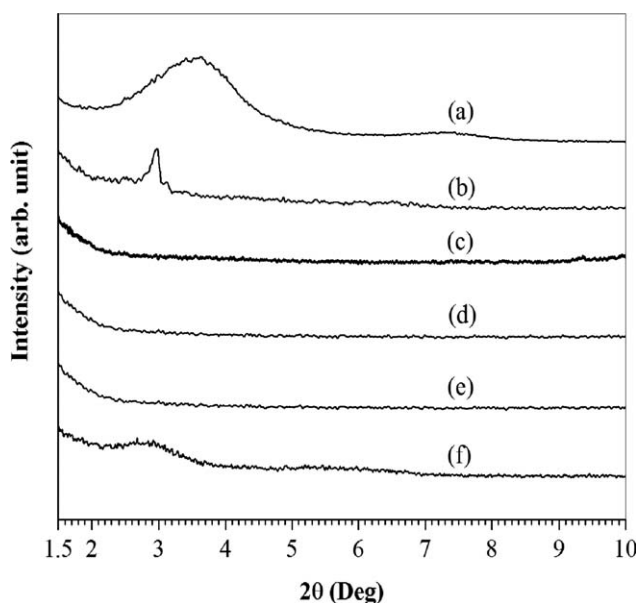


**Figure 4** WAXD patterns of the pure clay (a), and its composites: (b) HDPE-clay (1 phr); (c) nylon6-clay (1 phr); (d) 70/30 w/w nylon6/HDPE blend-clay (1 phr); (e) 30/70 w/w nylon6/HDPE blend-clay (1 phr); (f) 30/70 w/w nylon6/HDPE blend-clay (5 phr).

region ( $2.96^\circ$ ) in HDPE/clay (1 phr) nanocomposites indicated the intercalation of HDPE chains inside the clay galleries with a  $d$ -spacing of 2.98 nm. Whereas, absence of any clay peak in nylon6/clay (1 phr) nanocomposites indicated the exfoliation of clays in nylon6 matrix. Interestingly, absence of clay characteristic peaks in (70/30 and 30/70 w/w) nylon6/HDPE blends with 1phr clay indicated the exfoliation of the clay layers in nylon6. However, in (30/70 w/w) nylon6/HDPE blend with 5 phr of clay, a broad peak was observed at lower region ( $2\theta \approx 2.92^\circ$ ) which indicated the intercalation of clays ( $d_{001} \approx 3.02$  nm) in the blend. We assumed that, at higher clay loading (5 phr), along with the exfoliation of clays in nylon6 phase, discernible amount of clays were also intercalated in HDPE phase of the blend. Thus, clays were exfoliated in the nylon6 domains and intercalated in HDPE matrix of (30/70 w/w) nylon6/HDPE blend-clay (5 phr) nanocomposites.

The location of the clay platelets in the blend-clay nanocomposites was investigated by TEM analysis. Figure 5 represents the TEM images of the (70/30 w/w) nylon6/HDPE blend with clay (0.1 phr) at different magnifications. The matrix-droplet morphology of the blend was evident at low magnification [Fig. 5(a), at 5 kX]. TEM image at higher magnifications [Fig. 5(b,c), at 10 and 50 kX, respectively] clearly indicated the location of the clay platelets selectively in the nylon6 matrix. This preferential location of clay in nylon6 was due to the difference in polarity of nylon6 and HDPE. Nylon6 being polar

than HDPE, the clay layers tend to exfoliate and locate mostly in the nylon6 matrix in (70/30 w/w) nylon6/HDPE blend. However, it could not be excluded that discernible amount of intercalated clay platelets might also be located inside the HDPE domains at higher loading of clay in the blend.

On the basis of SEM, XRD and TEM observations of (70/30 w/w) nylon6/HDPE blend-clay nanocomposites, we assumed that the exfoliated clay platelets in nylon6 matrix acted as barriers that prevented the coalescence of dispersed HDPE domains during melt mixing. This resulted in finer dispersion of HDPE domains in nylon6 matrix, and hence reduction in HDPE domain sizes in the blend. Furthermore, the morphology of the (70/30 w/w) nylon6/HDPE blend was not stable against static annealing at  $250^\circ\text{C}$  for 4 h (Fig. 6). For instance, the  $D$  (2.84  $\mu\text{m}$ ) of (70/30 w/w) nylon6/HDPE blend was increased to  $\sim 3.8$   $\mu\text{m}$ , whereas the  $D$  of the blend with clay (0.1 phr) did not change significantly after annealing.

If the barrier effect of clay in matrix phase of (70/30 w/w) nylon6/HDPE blend played a key role in

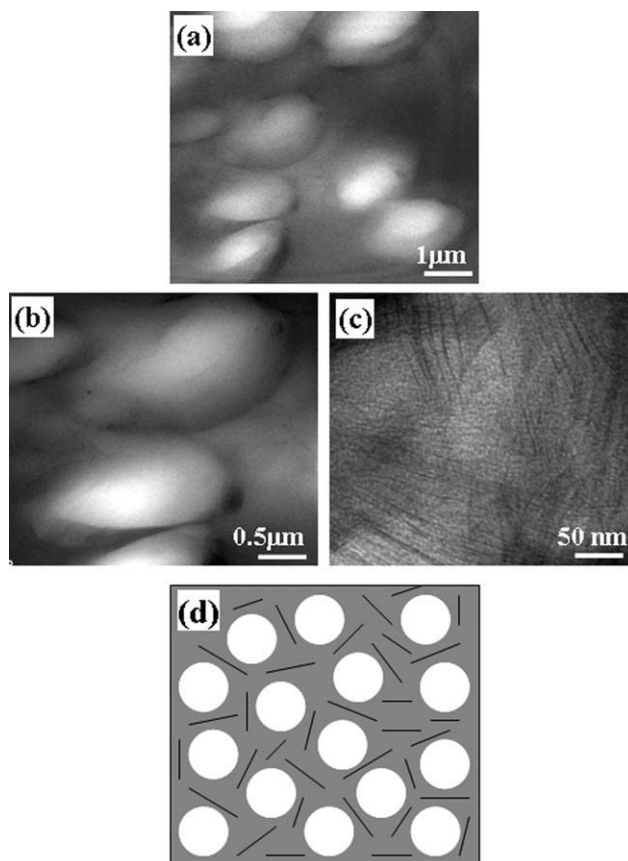


**Figure 5** TEM images of (70/30 w/w) nylon6/HDPE blend with clay (0.1 phr) at different magnifications: (a) low (5 kX) magnification, (b) HDPE domains at higher (10 kX) magnification, (c) nylon6 matrix at higher (50 kX) magnification, and (d) the schematic for location of clays in the blend.

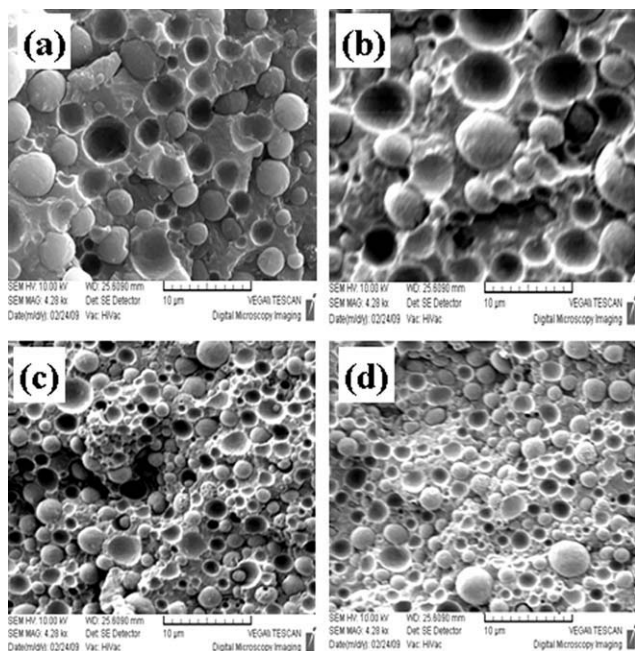


**Figure 6** SEM images of (70/30 w/w) nylon6/HDPE blends before (a and c) and after annealing (b and d): (a and b) pure blends; (c, d) blend with 0.1 phr clay. All the images were taken at same magnification, with a scale bar of 10  $\mu\text{m}$ .

reducing  $D$  of the blend then one can not expect same role of the clay in another blend system where clays were located in the domains only. For this, we considered the morphology of (30/70 w/w) nylon6/HDPE blend with clay (Fig. 7). Interestingly, addition of 0.5 phr of clay in this reverse blend system slightly increased the  $D$  of dispersed nylon6 phases [Fig. 7(b)]. The  $D$  of the blend increased progressively with increasing the loading of clay (not shown). This was due to the preferential location of clay inside the nylon6 domains (see WAXD section) that increased the viscosity of the dispersed phase. However, addition of PE-g-MA in this reverse blend decreased the  $D$  of dispersed HDPE domains [Fig. 7(c)]. Furthermore, the morphology of (30/70 w/w) nylon6/HDPE blend with clay (0.5 phr) was not stable upon static annealing [Fig. 7(d)]. This observation led us to conclude that absence of clay platelets in the matrix phase (HDPE) failed to prevent the coalescence of dispersed domains in (30/70 w/w) nylon6/HDPE blend-clay system.

The location of the clay silicate layers in the (30/70 w/w) nylon6/HDPE blend investigated by TEM analysis is shown in Figure 8. The dispersed nylon6 phase in the blend appeared as black domains [Fig. 8(a)] at low magnification. TEM images at higher magnification [Fig. 8(b)] clearly indicated the preferential location of the clay layers in side the dispersed nylon6 domains in this reverse blend-clay nanocomposites system. We assumed that the exfoliated clay

platelets in side the nylon6 domains in (30/70 w/w) nylon6/HDPE blend-clay system could not play the role of a barrier to prevent the coalescence of dispersed domains in HDPE matrix. This was also supported by the increase in  $D$  of this blend in presence of clay after annealing (see Fig. 7). Thus, no decrease in  $D$  was observed in this reverse blend even when the loading of clay was increased to 5 phr.

The barrier effect of the clay in the blend was also investigated with a highly asymmetric blend composition of nylon6/HDPE, where the probability of coalescence of the dispersed droplets was almost negligible (Fig. 9). For instance, the matrix/droplet morphology of (99/1 w/w) nylon6/HDPE blend [Fig. 9(a)] did not exhibit significant change in  $D$  of dispersed HDPE domains upon annealing at 250°C for 4h, indicating almost no coalescence of HDPE domains. The dispersed HDPE domains in this blend were located away from each other. We found that the  $D$  of the blend without any clay was (1.52  $\mu\text{m}$ ), which is significantly smaller than that (2.84  $\mu\text{m}$ ) of the (70/30 w/w) nylon6/HDPE blend. Interestingly,  $D$  of (99/1 w/w) nylon6/HDPE blend with 0.1 phr clay [Fig. 9(b)] was 1.48  $\mu\text{m}$ , which is almost the same as that without any clay. A slight decrease in  $D$  (1.26  $\mu\text{m}$ ) for the blend with 0.5 phr of the clay [Fig. 9(c)] was due to the increase viscosity of the matrix phase in presence of clay. However,  $D$  of the blend decreased to 0.98  $\mu\text{m}$  when 0.5 phr PE-g-MA

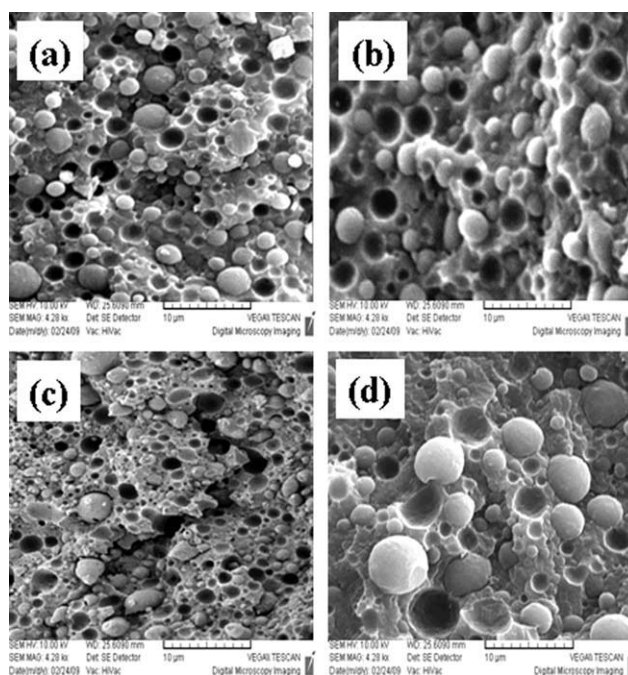


**Figure 7** SEM images of (30/70 w/w) nylon6/HDPE blend (a), and the blend with: (b) 0.5 phr clay, (c) 0.5 phr PE-g-MA, and (d) represents the image of (b) after annealing. All the images were taken at same magnification, with a scale bar of 10  $\mu\text{m}$ .

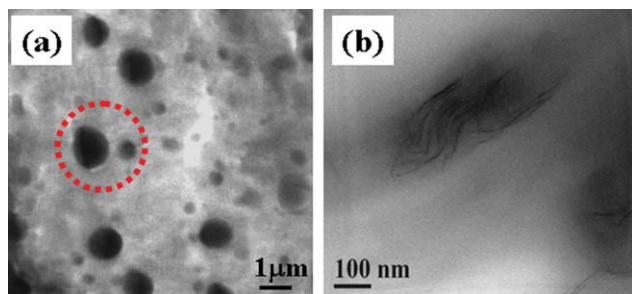


**Figure 8** TEM images of (30/70 w/w) nylon6/HDPE blend with clay (0.5 phr) at different magnifications: (a) low magnification, (b) nylon6 domain at higher magnification. [Color figure can be viewed in the online issue, which is available at [wileyonlinelibrary.com](http://wileyonlinelibrary.com).]

was added into the blend [Fig. 9(d)]. This observation clearly indicated that the role played by the clay silicates in reducing *D* of nylon6/HDPE blend was not similar to that of block (or graft) copolymers as compatibilizer in immiscible polymer blends.

**Effect of matrix viscosity on the morphology**

The decrease in *D* of (70/30 w/w) nylon6/HDPE blend in presence of clay might also result from the increase viscosity of the matrix phase, as clay platelets were selectively dispersed in the nylon6 phase. Assuming all the clays in (70/30 w/w) nylon6/HDPE blend-clay (0.1 phr) system located selectively in nylon6 phase, the effective loading of clay in nylon6 was 0.14 phr. Figure 10 represents the complex

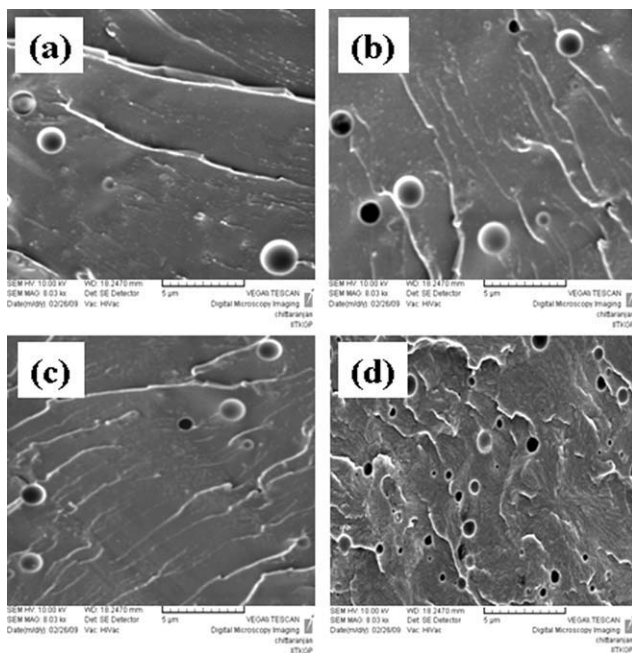


**Figure 9** SEM images of (99/1 w/w) nylon6/HDPE blend (a), and the blend with: (b) 0.1 phr clay, (c) 0.5 phr clay, and (d) 0.5 phr PE-g-MA. All the images were taken at same magnification, with a scale bar of 5 μm.

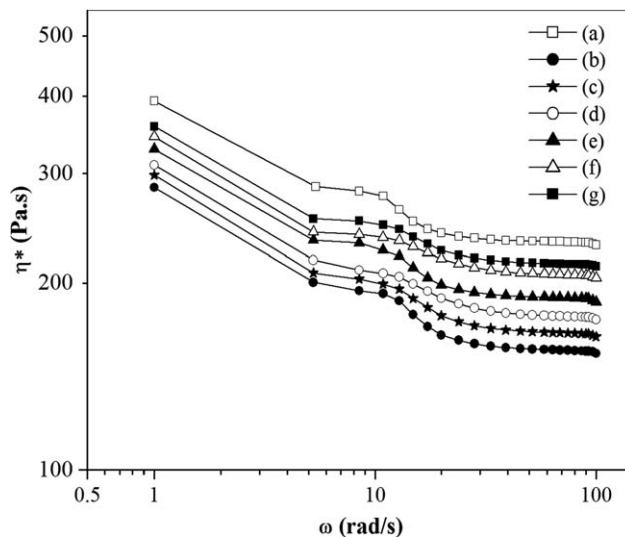


**Figure 10** Plot of complex viscosity ( $\eta^*$ ) with frequency ( $\omega$ ) at 250°C: (a) HDPE; (b) nylon6; (c) nylon6-clay (0.14 phr); (d) nylon6-h; (e) 70/30 (w/w) nylon6/HDPE blend; (f) 70/30 (w/w) nylon6/HDPE blend with 0.1 phr clay; and (g) 70/30 (w/w) nylon6-h/HDPE blend without any clay.

viscosity ( $\eta^*$ ) of nylon6 and its nanocomposites with 0.14 phr clay. As observed,  $\eta^*$  of nylon6 increased marginally by the addition of 0.14 phr clay. To clarify the effect of matrix viscosity on the morphology of nylon6/HDPE blend with 0.1 phr clay, we considered (70/30 w/w) nylon6/HDPE blend with a high viscosity nylon6 (nylon6-h), as shown in Figure 10. The  $\eta^*$  of nylon6-h was higher than that of nylon6 and almost similar to the viscosity ( $\eta^*$ ) of nylon6/clay (0.14 phr) nanocomposites at the entire frequency region (0.1–100 rad s<sup>-1</sup>).

We observed that (Fig. 11) the *D* of (70/30 w/w) nylon6-h/HDPE blend was 2.46 μm, which was slightly smaller than that (2.84 μm) of the (70/30 w/w) nylon6/HDPE blend. But the *D* of nylon6/HDPE blend with 0.1 phr clay was 2.06 μm (Fig. 1), which was much lower than that (2.46 μm) in nylon6-h/HDPE blend, although the complex viscosity ( $\eta^*$ ) of

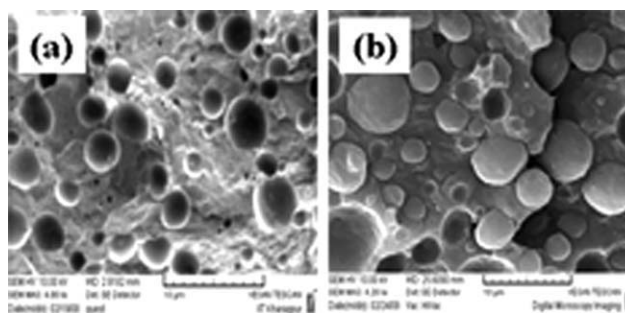


**Figure 11** SEM images of (70/30 w/w) nylon6-h/HDPE blends before annealing (a), and after annealing (b). All the images were taken at same magnification, with a scale bar of 10 μm.

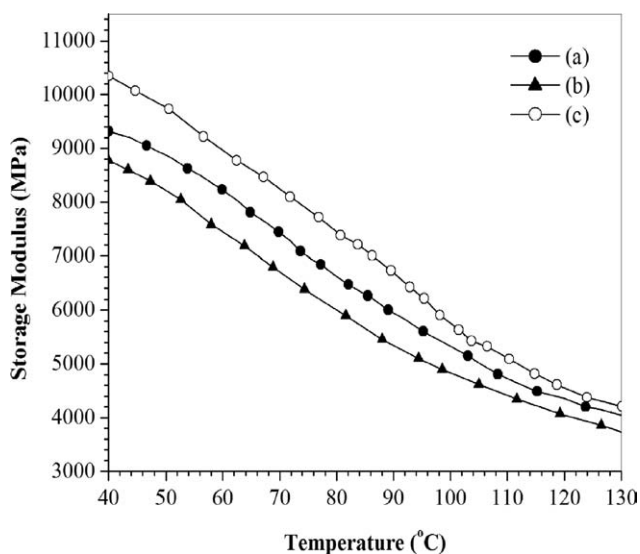


**Figure 12** Storage modulus of (70/30 w/w) nylon6/HDPE blend (a), and the blend with (b) 1 phr of PE-g-MA, (c) 0.1 phr of clay.

the later blend was even higher than the former one. Moreover, when (70/30 w/w) nylon6-h/HDPE blend was annealed at 250°C for 4 h,  $D$  of the blend increased to 3.92  $\mu\text{m}$ . Thus, the morphology of nylon6-h/HDPE blends was not stable against annealing. Whereas, the  $D$  of nylon6/HDPE blend with clay (0.1 phr) was almost unaffected after annealing under the same condition (see Fig. 6). These results clearly indicated that the exfoliated clay platelets in the matrix phase (nylon6) played the role of a barrier that prevented the coalescence of dispersed HDPE domains in nylon6/HDPE blend.

### Mechanical properties

Figure 12 represents the storage modulus of (70/30 w/w) nylon6/HDPE blend without and with PE-g-MA or clay. We found that  $D$  of the blend with 0.1 phr clay was 2.06  $\mu\text{m}$ , which is almost similar to the  $D$  (1.98  $\mu\text{m}$ ) of the blend with 1 phr PE-g-MA. However, storage modulus of the pure blend ( $D \approx 2.84 \mu\text{m}$ ) decreased significantly when 1 phr PE-g-MA was added into the blend, although  $D$  of the blend in the later case (1.98  $\mu\text{m}$ ) was smaller. Interestingly, (70/30 w/w) nylon6/HDPE blend with 0.1 phr of the clay showed higher storage modulus than that of the pure blend, as well as, the blend with 1 phr of PE-g-MA having comparable  $D$  value. Thus, PE-g-MA reduced the stiffness of the blend, consistent with the earlier report.<sup>21</sup> Whereas, the reinforcing effect of the high aspect ratio stiff clay silicates increased the stiffness of the blend.

The storage modulus of (30/70 w/w) nylon6/HDPE blend and that with the clay or PE-g-MA is shown in Figure 13. As observed, addition of 1 phr

PE-g-MA significantly decreased the storage modulus of the blend. Whereas, the blend with small amount (0.1 phr) of clay showed improvement in storage modulus compared to the pure blend. It's noteworthy that the improvement in storage modulus of nylon6/HDPE blend in presence of clay (0.1 phr) was more in case of (70/30 w/w) nylon6/HDPE blend than that of (30/70 w/w) nylon6/HDPE blend. We assumed that, the exfoliation of clays in nylon6 matrix of (70/30 w/w) nylon6/HDPE blend resulted in a maximum interaction of the polymer chains (70 wt % nylon6) with the clay platelets compared to that in the case of (30/70 w/w) nylon6/HDPE blend where clays were exfoliated in nylon6 domains (30 wt % nylon6).

### Tensile properties

Tensile strength and elongation properties of (70/30 and 30/70 w/w) nylon6/HDPE blends without and with clay or PE-g-MA, are shown in Table I. As evident, incorporation of clay up to 1 phr increased the tensile strength for both compositions of the blend. The improvement in tensile strength in presence of clay was due to the reinforcing effect of exfoliated clay silicate layers in the blends. At higher loading of clay (at and above 3 phr), tensile strength of the blends decreased and approached to that of the pure blends when 5 phr clay was added to the blend. This might be due to the agglomeration or poor dispersion of the clay silicates in the nylon6 phase at higher clay loading that lowered the tensile property of the blends. However, addition of clay drastically decreased the elongation at break of nylon6/HDPE blend for both (70/30 and 30/70 w/w)

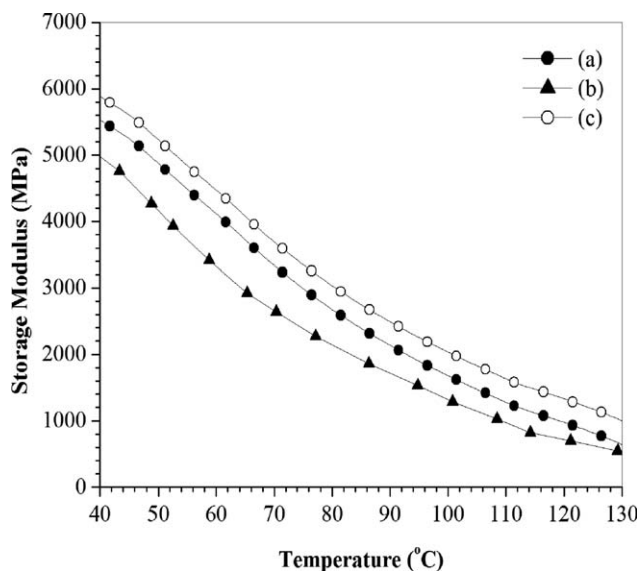


**Figure 13** Storage modulus of (30/70 w/w) nylon6/HDPE blend (a), and the blend with (b) 1 phr of PE-g-MA, (c) 0.1 phr of clay.



**TABLE I**  
**Tensile Strength and Elongation at Break of Nylon6/HDPE Blends with Different Amount of Clay and PE-g-MA**

Sample details	Tensile strength (MPa)	Elongation at break (%)
(70/30 w/w) Nylon6/HDPE	21.67 ± 2.3	14.4 ± 1.7
(70/30 w/w) Nylon6/HDPE with 0.1 phr clay	23.48 ± 1.8	13.6 ± 1.5
(70/30 w/w) Nylon6/HDPE with 0.5 phr clay	25.89 ± 2.5	14.2 ± 1.4
(70/30 w/w) Nylon6/HDPE with 1 phr clay	30.75 ± 3.2	13.2 ± 1.5
(70/30 w/w) Nylon6/HDPE with 3 phr clay	24.66 ± 2.1	12.2 ± 1.6
(70/30 w/w) Nylon6/HDPE with 5 phr clay	21.74 ± 2.6	10.3 ± 1.5
(70/30 w/w) Nylon6/HDPE with 0.1 phr PE-g-MA	20.24 ± 1.9	16.8 ± 1.6
(70/30 w/w) Nylon6/HDPE with 0.5 phr PE-g-MA	19.76 ± 2.5	21.3 ± 1.4
(70/30 w/w) Nylon6/HDPE with 1 phr PE-g-MA	18.23 ± 2.4	24.5 ± 1.5
(70/30 w/w) Nylon6/HDPE with 3 phr PE-g-MA	17.50 ± 2.8	31.7 ± 1.8
(70/30 w/w) Nylon6/HDPE with 5 phr PE-g-MA	15.66 ± 1.4	32.0 ± 1.3
(30/70 w/w) Nylon6/HDPE	17.28 ± 1.4	12.5 ± 1.2
(30/70 w/w) Nylon6/HDPE with 0.5 phr clay	20.42 ± 2.5	10.0 ± 1.4
(30/70 w/w) Nylon6/HDPE with 1 phr clay	26.92 ± 2.3	8.5 ± 1.3
(30/70 w/w) Nylon6/HDPE with 3 phr clay	24.87 ± 2.3	5.8 ± 1.5
(30/70 w/w) Nylon6/HDPE with 5 phr clay	16.54 ± 2.3	5.1 ± 1.3

the compositions, indicating lack of adhesion between the polymers at the interface in the blend. The reduction in ductility was attributed to the constrained mobility of polymer chains in presence of the clay particles.

Addition of PE-g-MA showed reverse effect on the tensile properties of (70/30 w/w) nylon6/HDPE blend, compared to that with clay in the blend. The tensile strength of the blend decreased with the PE-g-MA content. However, elongation at break of the blend increased significantly when small amount (0.5 phr) of PE-g-MA was added into the blend. PE-g-MA is well known to act as reactive compatibilizer for the blend that improves the adhesion between nylon6 and HDPE chains through formation of PE-g-nylon6 at the interface.<sup>22</sup>

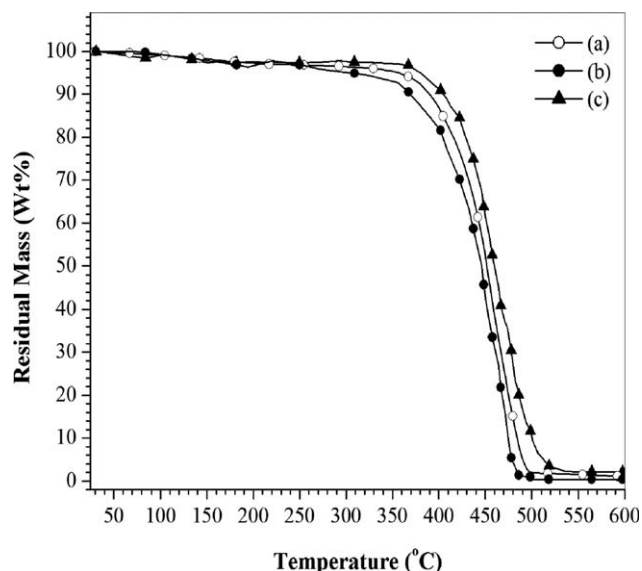
### Thermal analysis

Figure 14 represents the TGA scans for (70/30 w/w) nylon6/HDPE blend and the blends with the clay (0.1 phr) or PE-g-MA (1phr). As observed, tempera-

ture corresponds to 10 wt % loss ( $T_{10}$ ) of the pure blend ( $D \approx 2.84 \mu\text{m}$ ) was 387°C, which is higher than that (365°C) of the blend ( $D \approx 1.98 \mu\text{m}$ ) with 1 phr PE-g-MA. Interestingly, the degradation temperature ( $T_{10} \approx 405^\circ\text{C}$ ) of (70/30 w/w) nylon6/HDPE blend with 0.1 phr of the clay ( $D \approx 2.06 \mu\text{m}$ ) was significantly high compared to the pure blend, as well as, PE-g-MA containing blend having comparable  $D$  values. The degradation temperatures correspond to 50% weight loss ( $T_{50}$ ) and maximum weight loss ( $T_{\text{max}}$ ) of the blend were also increased in presence of small amount (0.1 phr) of clay. Whereas, incorporation of PE-g-MA (1 phr) lowered the  $T_{50}$  and  $T_{\text{max}}$  values of the pure blend indicating decrease in thermal stability in the blend. The improvement in thermal stability of the blend in the presence of clay could be associated with the inorganic clays having high thermal stability and thermal barrier properties that prevented the diffusion of heat into the bulk. This led to an increase in the decomposition temperatures of the blend at different stages, in presence of clay.

### CONCLUSIONS

This investigation shows the role of organoclay on the morphology and properties of immiscible nylon6/HDPE blends. The average domain size ( $D$ ) of the dispersed HDPE phase in (70/30 w/w) nylon6/HDPE blend decreased significantly even at lower loading (0.1 phr) of clay. For a particular loading, reduction in  $D$  of dispersed HDPE phase in nylon6/HDPE blend was more significant with the clay than that with PE-g-MA. However, the same effect of the



**Figure 14** TGA scans for (70/30 w/w) nylon6/HDPE blend (a) and the blend with (b) 1 phr of PE-g-MA, (c) 0.1 phr of clay.

clay was not observed when HDPE became the matrix phase in nylon6/HDPE blend. Microscopic analysis of (70/30 w/w) nylon6/HDPE blends with the clay indicated localization of the exfoliated clay silicates selectively in the nylon6 matrix phase. Thus, nanoclay played the role of a compatibilizer for this blend as long as the clay platelets were dispersed in the matrix phase. The increase in  $D$  of HDPE after annealing in case of high viscosity nylon6/HDPE blend without any clay indicated that the increase viscosity of the matrix (nylon6) phase in presence of clay did not play a major role in reducing the  $D$  of (70/30 w/w) nylon6/HDPE blend. Again, no significant change in  $D$  of HDPE after annealing in nylon6/HDPE with clay led us to conclude that the exfoliated clay platelets in the matrix phase of the blend acted as barriers that prevented the coalescence of dispersed domains during melt-mixing and thus, reduced the dispersed domain sizes in the blend. Moreover, a decrease in elongation property of the blend in presence of clay revealed that the clay did not promote any adhesion between the phases in the blend.

## References

1. Folkes, M. J.; Hope, P. S. *Polymer Blends and Alloys*; Blackie Academic and Professional An imprint of Chapman & Hall: UK, 1993.
2. Utracki, L. A.; *Polymer Alloys and Blends*, Hanser Publishers: Munich, Germany, 1989.
3. Creton, C.; Kramer, E. J.; Hui, C.-Y.; Brown, H. R. *Macromolecules* 1992, 25, 3075.
4. Kim, S.-J.; Shin, B.-S.; Hong, J.-L.; Cho, W.-J.; Ha, C.-S. *Polymer* 2001, 42, 4073.
5. Boucher, E.; Folkers, J. P.; Hervet, H.; Léger, L.; Creton, C. *Macromolecules* 1996, 29, 774.
6. Khatua, B. B.; Lee, D. J.; Kim, H. Y.; Kim, J. K. *Macromolecules* 2004, 37, 2454.
7. Hong, J. S.; Namkung, H.; Ahn, K. H.; Lee, S. J.; Kim, C. *Polymer* 2006, 47, 3967.
8. Gelfer, M. Y.; Hyun, H. S.; Liu, L.; Benjamin, S. H.; Benjamin, C.; Rafailovich, M.; Mayu, S.; Vladimir, Z. *J Polym Sci Part B* 2003, 41, 44.
9. Wang, Y.; Zhang, Q.; Fu, Q. *Macromol Rapid Commun* 2003, 24, 231.
10. Sinha Ray, S.; Bousmina, M. *Macromol Rapid Commun* 2005, 26, 450.
11. Sinha Ray, S.; Bousmina, M. *Macromol Rapid Commun* 2005, 26, 1639.
12. Sung, Y. T.; Kim, Y. S.; Lee, Y. K.; Kim, W. N.; Lee, H. S.; Sung, J. Y.; Yoon, H. G. *Polym Eng Sci* 2007, 47, 1671.
13. Gwabaza, T.; Sinha Ray, S.; Focke, W. W.; Maity, A. *Euro Polym J* 2009, 45, 353.
14. Mehta, S.; Mirabella, F. M.; Rufener, K.; Bafna, A. *J Appl Polym Sci* 2004, 92, 928.
15. Kelnar, I.; Rotreki, J.; Kotek, J.; Kapralkova, L. *Polym Int* 2008, 57, 1281.
16. Calcagno, C. I. W.; Mariani, C. M.; Teixeira, S. R.; Mauler, R. S. *Compos Sci Technol* 2008, 68, 2193.
17. Filippone, G.; Dintcheva, N. Tz.; Acierno, D.; Mantia, F. P. *La Polymer* 2008, 49, 1312.
18. Fang, Z.; Xu, Y.; Tong, L. *Polym Eng Sci* 2007, 47, 551.
19. González, T. V.; Salazar, C. G.; De La Rosa, J. R.; González, V. G. *J Appl Polym Sci* 2008, 108, 2923.
20. Favis, B. D. *Polymer* 1994, 35, 1552.
21. Kusmono, Z. A.; Mohd Ishak, W. S.; Chow, T.; Takeichi, R. *Compos Part A Appl Sci Manufact* 2008, 39, 1802.
22. Agrawal, P.; Rodrigues, A. W. B.; Araujo, E. M.; Melo, T. J. A. *J Mater Sci* 2010, 45, 496.